1-15-2021

# Addressing the Practical Limitations of Volatile Organic Compound Sensors Through an Oscillator-Based Sensing Array

Allison K. Murray

Joseph R. Meseke

Nikhil Bajaj

Jeffrey F. Rhoads

*IEEE Sensors Journal*, Vol. 21, No. 2 (January 15, 2021): 2169-2175. DOI. 

# Addressing the Practical Limitations of Volatile Organic Compound Sensors Through an Oscillator-Based Sensing Array

Allison K. Murray
School of Mechanical Engineering, College of Engineering, Purdue University, West Lafayette, IN
Ray W. Herrick Laboratories, Purdue University, West Lafayette, IN
Joseph R. Meseke
School of Mechanical Engineering, College of Engineering, Purdue University, West Lafayette, IN
Ray W. Herrick Laboratories, Purdue University, West Lafayette, IN
Nikhil Bajaj
School of Mechanical Engineering, College of Engineering, Purdue University, West Lafayette, IN
Ray W. Herrick Laboratories, Purdue University, West Lafayette, IN
Birck Nanotechnology Center, Purdue University, West Lafayette, IN
Jeffrey F. Rhoads
School of Mechanical Engineering, College of Engineering, Purdue University, West Lafayette, IN

Ray W. Herrick Laboratories, Purdue University, West Lafayette, IN
Birck Nanotechnology Center, Purdue University, West Lafayette, IN

## Abstract:

This work demonstrated the development of an array of oscillator-based sensors for the detection of volatile organic compounds (VOCs). A field-programmable gate array (FPGA) was leveraged to monitor the oscillation frequency of 16 sensing elements in parallel. It was shown that three functional chemistries can be deposited via inkjet printing to detect several analytes selectively. These unique response characteristics allowed for the creation of a linear regression model that relates the shifts in oscillation frequencies to the concentration of specific analytes. This approach utilized a single array with sufficient elements to incorporate intentional redundancies. Ultimately, this work demonstrated a low-cost oscillator-based sensing array capable of simultaneously monitoring chemical processes with single second resolution using 16 independent channels.

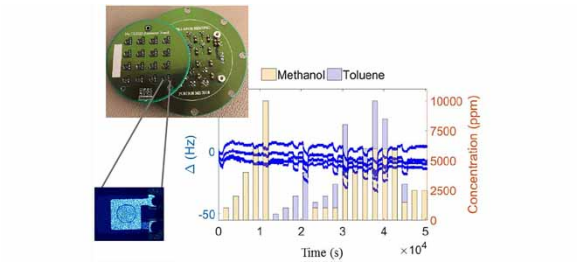


## **SECTION I.** Introduction

As society spends more time indoors, the exposure to volatile organic compounds (VOCs) released by building materials, coatings, and colorants, amongst other common sources, becomes more prevalent. VOCs are chemicals with high vapor pressures at room temperature and are often detrimental to human health [1]. As regulations and safety concerns increase, the need for reliable, sensitive, and selective VOC sensors is pressing. Lab-based sensing advancements have shown promise for VOC detection [2]–[3][4]. However, most of these technologies struggle to span the valley of death associated with transforming research successes to market-ready products. A major factor in this lack of technology transfer is the difference between bench-top detection claims and predictions of species concentrations in realistic environments. Extensive work has been done to develop portable VOC sensors with detection limits in the low parts-per-million to hundreds of parts-per-billion range [3], [5], [6]. However, there has been comparatively little work focused on accurately extrapolating the concentration of a specific analyte directly from the sensor's voltage or frequency output [2], [4]. For practical implementation, sensing platforms should be designed to maximize predictive capabilities without compromising detection limits [7]–[8][9]. For example, sensor development must move beyond reporting detection as a change in frequency or resistance and towards estimating multi-analyte concentration based on those values.

There has been extensive research on metal-oxide chemiresistive VOC sensors with parts-per-million sensitivity [5]. These resistive sensors require high operational temperatures, and thus appreciable power budgets. This results in cumbersome and/or costly sensor integration. Additionally, reviews of the subject have concluded there exists a need for a more selective, not just sensitive, approach when identifying specific analytes of interest [5]. Electronic-nose arrays are capable of identifying analytes

through large data set processing, but require an appreciable number of sensors to gain information [10], [11]. Furthermore, these sensor networks typically lack quantitative information regarding analyte concentration and are unable to identify individual chemical gas components [3], [10]. To practically implement selective VOC sensors, low-cost platforms with multi-analyte concentration estimation tools are needed.

This work utilized a multi-channel oscillator-based sensing array with a frequency counting algorithm to address the aforementioned limitations in current sensing capabilities. Oscillators have previously been used as the sensing element in mass detection across various applications to achieve sensitive detection at a low cost [12]–[13][14][15]. In this work, a field programmable gate array (FPGA) based frequency counter was used to simultaneously monitor 16 sensing channels in parallel. Previous work has leveraged frequency counting to monitor the oscillation frequency of mass sensors [16]. Similarly, shifts in the resonance frequency of MEMS resonators and quartz crystal microbalances (QCM) have been quantified using frequency counting for the detection of VOCs in power-efficient devices [17], [18].

The oscillators in this work were functionalized via inkjet printing for tailored manufacturing. This allowed for the deposition of multiple materials across a single sensing array. This manufacturing approach has been used with appreciable success in prior work to precisely deposit a functional chemistry onto the sensing element [17], [19]–[20][21][22]. Through inkjet printing, the amount of functional chemistry and the area of functionalization can be tuned to enable high sensitivity without compromising the nature of oscillation by adding too much mass or damping.

By leveraging 16 parallel channels with redundant elements, simultaneous data collection, and 1 s temporal resolution, a non-trivial amount of frequency shift and concentration level data was collected. This approach facilitated the development of a preliminary linear regression model of ambient air concentration with multiple analyte selectivity. The sensing array demonstrated herein can provide a first step towards predicting resonant mass detection limits based off of large data sets. This work also helps assist laboratory sensors in the translation into practical field implementation with similar performance.

## **SECTION II.** Materials and Methods

### A. Sensor Design and Fabrication

A sensor array of 16 Pierce oscillators (see Figure 1) was fabricated for this work. Each oscillator consisted of an inverter, two load capacitors, $C_1$ = 22 pF and $C_2$ = 22 pF, one feedback resistor, R1=2MΩ , one isolation resistor, R2=510Ω , and a 16 MHz quartz crystal resonator (Kyocera Corp., CX3225), CL=12 pF. The crystal oscillator driver, COD (Texas Instruments, SN74LVC1GX04), provided the circuit with the Pierce oscillator inverter, as well as three additional inverters which converted the oscillator output signal to a square wave. The hardware implementation of the oscillator circuit resulted in two printed circuit boards: a board with solely an array of resonators and an instrumentation board containing the remaining elements of the oscillator circuit (see Figure 1). The resonator board was secured to the instrumentation board such that spring connection pins provided the necessary electrical coupling to place the resonator within the oscillator circuit. Given this, the

resonator boards could be interchanged quickly and without incurring high component costs. The instrumentation board also served as the bottom of the 9.5 cm diameter test chamber.

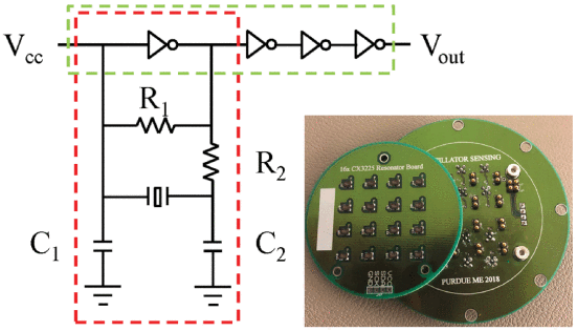


**Fig. 1.** A Pierce oscillator circuit with the oscillator (red) and a series of inverters (green) depicted along with the resonator board and instrumentation board offset to show electrical connections.

A frequency counter was implemented to monitor the oscillation frequency of each device in parallel, a schematic of which is shown in Figure 2. The instances of the rising edge of the oscillator output voltage were counted. The number of rising edges per second was reported as the oscillation frequency. Because this method required multiple analyses for each cycle of the input signal, the frequency counter loop needed to run significantly faster than 16 MHz, the nominal oscillation frequency of the devices. To achieve the computational speeds required, the frequency counter was synthesized and executed on a National Instruments myRio field-programmable gate array (FPGA) with a 120 MHz internal clock. The FPGA allowed for parallel computing on all 16 channels.

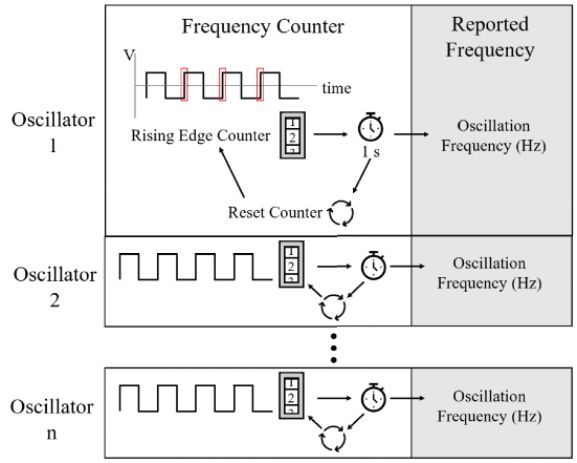


**Fig. 2.** A graphical representation of the frequency counting method to accept 16 oscillator outputs and compute the corresponding oscillation frequencies every second with 1 Hz resolution.

## B. Sensor Functionalization

A BioFluidix PipeJet P9 piezoelectrically actuated pipette with a 200 µm nozzle was used to deposit 5 nL of a functional ink onto each quartz resonator. A machine vision and spatial registration system was implemented with a high-precision linear axis stage (AeroTech PlanarDL-200-XY) to deposit the material at the center of the device to maximize sensitivity [22]. A representative image of a resonator before and after functionalization is shown in Figure 3. The three polymers detailed in Table I were chosen as the solutes in this work due to their previously demonstrated sensitivities to volatile organic

compounds [23]. The inks were randomly assigned to resonator locations and additional resonators were left unfunctionalized to serve as temperature and humidity references. After functionalization, the resonator board was stored under vacuum for a minimum of 24 hr to remove any remaining solvent.

**TABLE I** Functional Chemistries Inkjet Printed on the Resonators at 5 nL Per Device. All of the Solvents and Polymer Were Sourced from Sigma Aldrich

| Solvent | Polymer | Concentration (mg/mL) |
|---|---|---|
| Toluene | Polymethylmethacrylate | 1 |
| Toluene | Polystyrene | 0.3 |
| Ethanol | Poly(4-vinylpyridine) | 1 |

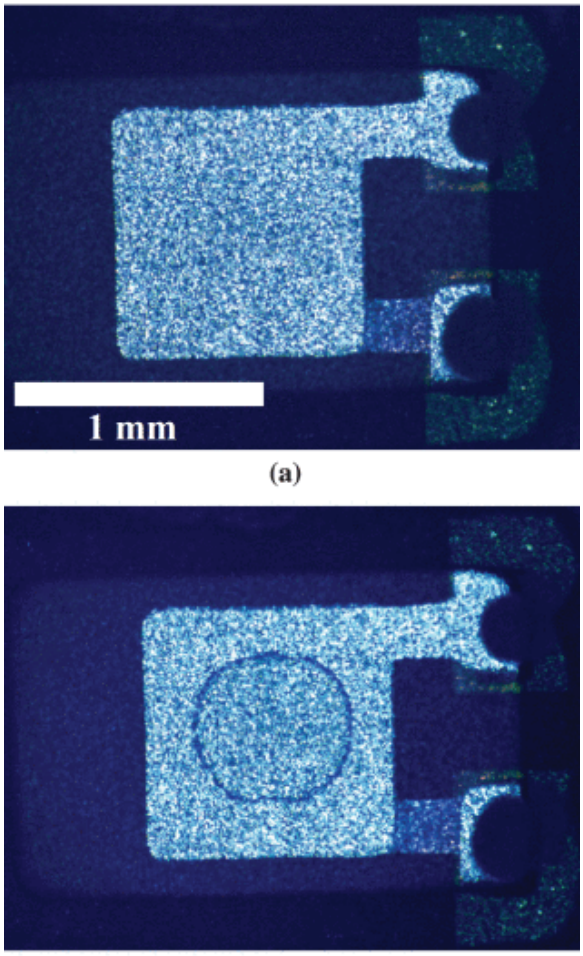


**Fig. 3.** Representative view of a resonator (a) before and (b) after functionalization. Note the center of the resonator is coated with a thin film of poly(4-vinylpyridine).

## C. Sensor Testing

Immediately prior to testing, the resonator board was secured to the instrumentation board and the chamber was sealed. The chamber was secured with an inline flow distribution system (see Figure 4) to achieve the desired concentrations of the analytes. Nitrogen was connected to three mass flow

controllers (MFCs) in parallel. Two of the MFCs (MKS 1480A, 40 ccm) were connected to bubblers (Chemglass, AF-0085) with either 10 mL of methanol or toluene. The other line (MKS 1179A, 500 ccm) remained a pure nitrogen source. The three inlets were connected to a manifold, the output of which was connected directly to the chamber inlet.

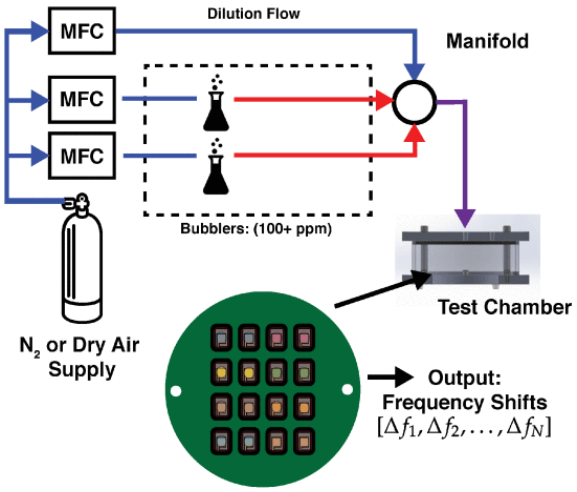


**Fig. 4.** Schematic representation of the experimental apparatus used for oscillator-based VOC sensing.

The chamber was flushed with pure nitrogen at 150 ccm to create an inert environment, which was used as the baseline for experimentation. Subsequently, the analyte gas was injected into the chamber to achieve the desired concentrations. Concurrently, the oscillation frequencies were recorded every second.

## SECTION III. Results

An array of 16 oscillators was fabricated such that four resonators were left unfunctionalized and three sets of four resonators were functionalized with 5 nL of an ink from Table I. The oscillation frequency recorded as a function of time for each set of devices is shown in Figure 5. The data is presented as a shift from the initial oscillation frequency, nominally 16 MHz. The stacked color bars represent the makeup of the gas flowing into the chamber at 150 ccm with yellow and purple indicating the concentration of methanol and toluene, respectively. To show the resolution achieved with this approach, a 65 min data subset of a single channel reported in Figure 5 is presented in Figure 6.

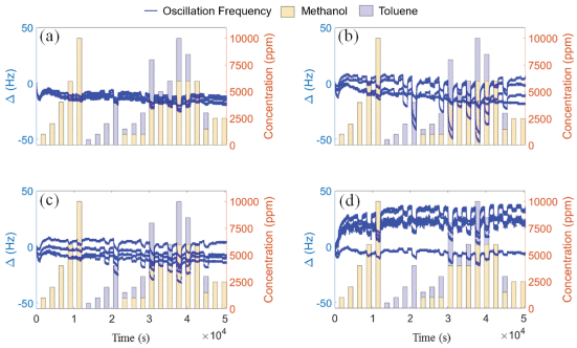


**Fig. 5.** The oscillation frequencies of 16 oscillators reported as shifts from the initial frequencies. The four devices in (a) were left unfunctionalized as a reference channel. Three groups of four resonators were functionalized with one of the following: (b) 1 mg/mL of polymethylmethacrylate in toluene, (c) 0.3 mg/mL of

polystyrene in toluene, and (d) 1 mg/mL of poly(4-vinylpyridine) in ethanol. The stacked color bars represent a makeup of the inlet gas at 150 ccm where yellow and purple indicate the methanol and toluene concentrations, respectively.

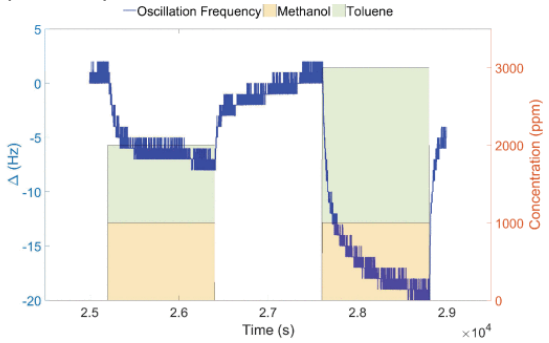


**Fig. 6.** A subset of a single channel presented in Figure 5 to demonstrate the resolution achievable with the presented sensing method. This device was functionalized with polymethylmethacrylate.

A linear regression model relating frequency shifts and analyte concentration was created. The frequency shift for each oscillator during every analyte exposure event was recorded as the difference in frequency of the oscillator 3 min before and 15 min after the analyte pulse was initiated. Shifts due to methanol and toluene concentrations ranging from 4000 to 14000 ppm were used as a training data set. The set was divided into n=4 subsets according to the functional ink. A linear regression model of the form:

$$\delta\Omega_1 = a_{1,0} + a_{1,1}M + a_{1,2}T$$
$$\ldots$$
$$\delta\Omega_n = a_{n,0} + a_{n,1}M + a_{n,2}T$$

was developed, where δΩi is the frequency shift of an oscillator functionalized with the ith ink, M is the concentration of methanol (ppm), and T is the concentration of toluene (ppm). Additional model terms that were not included due to a lack of predictive significance included resonator location; resonator number; concentration cross terms (e.g., M∗T ); higher-order concentration terms (e.g., M2 ); and the functional material's position on the resonator. The effect of the aforementioned terms was determined to be negligible through an ANOVA test. The training data set produced four regression equations, a unique equation for each ink in Table I and an equation for the reference channels. The regression coefficients and the coefficients of determination (R2 ) for these four models are presented in Table II.

**TABLE II** Linear Regression Coefficients and Coefficients of Determination for Each Ink Grouping Where PMMA is Polymethylmethacrylate and P4VP is Poly(4-Vinylpyridine)

| Material | Intercept $a_{n,0}$ (Hz) | Methanol $a_{n,1}$ (Hz/ppm) | Toluene $a_{n,2}$ (Hz/ppm) | $R^2$ |
|---|---|---|---|---|
| Reference | 1.5 | $-0.4 \cdot 10^{-4}$ | $-1.7 \cdot 10^{-3}$ | 0.98 |
| PMMA | 0.3 | $-7.2 \cdot 10^{-4}$ | $-3.7 \cdot 10^{-3}$ | 0.48 |
| Polystyrene | 2.3 | $-5.2 \cdot 10^{-4}$ | $-2.9 \cdot 10^{-3}$ | 0.75 |
| P4VP | 0.2 | $-13 \cdot 10^{-4}$ | $-2.5 \cdot 10^{-3}$ | 0.87 |

A new experimental data set with analyte exposure limits within the same range as the training data set was used to test the model. The frequency shifts of the 16 devices were known and the methanol and toluene concentrations for each pulse were predicted. Due to the over-constrained nature of the data set (i.e. 16 known shifts but only 2 unknown concentrations) a generalized inverse, or least squares approach, was used to invert the coefficient matrix and solve for M and T . To show the accuracy of the model, the experimental concentration was plotted against the predicted concentration in Figure 7 with the black line indicating an ideal fit. The methanol and toluene concentrations were predicted with an R2 of 0.81 and 0.99, respectively. The residuals of the methanol and toluene model are shown in Figure 8. These preliminary results suggest a first step at using redundant training data to predict the analyte concentration based on frequency shifts of functionalized resonators.

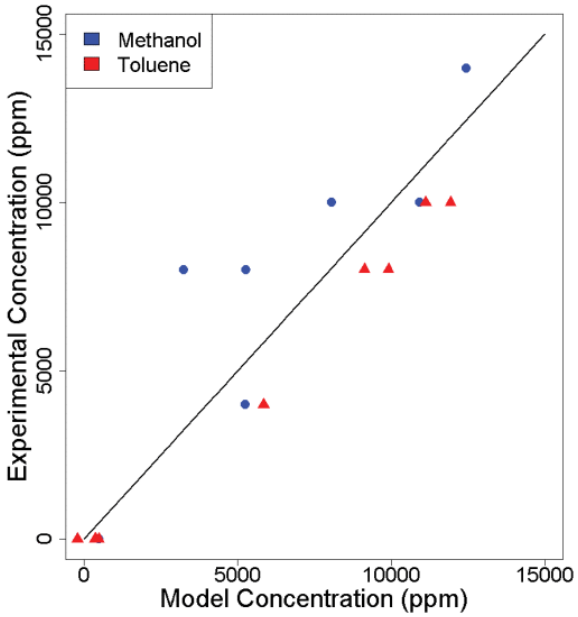


**Fig. 7.** The actual concentration level of methanol (blue) and toluene (red) plotted against the predicted analyte concentration. An ideal fit would follow the black line.

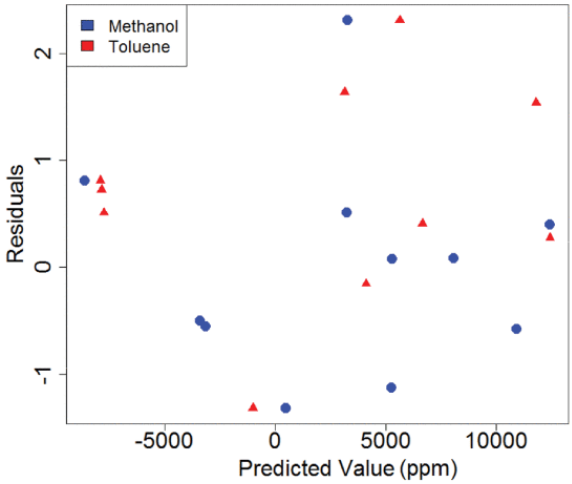


**Fig. 8.** The residuals of methanol (blue) and toluene (red) plotted against the predicted analyte concentration.

## **SECTION IV.** Discussion and Conclusion

It can be seen from Figure 5 that the time response of 16 oscillators can be monitored in parallel with this method. This approach generated an appreciable amount of data with 16 parallel channels reporting oscillation frequency once per second. This data provided a real-time picture of the system performance with realistic adsorption and desorption timescales. The data in Figure 5 includes an initial drift period of 20 min as the system reached an equilibrium under gas flow and temperature changes. This is of importance as implementation would require sufficient equilibration time. Additionally, Figure 6 demonstrated the timescale at which adsorption and desorption occurred in this system. All of the shift data used herein was presented when the system was at steady state, 15 min after the analyte pulse began. When considering practical implementation, the definition of steady state for concentration calculations would need to be defined.

In this work, the shift in oscillation frequency due to the addition of nitrogen, methanol, or toluene is different for each type of functional chemistry. When grouped by the functional ink, a one-way ANOVA test showed statistically significant differences in oscillation frequency shifts due to the addition of methanol, toluene, or a mixture there of. The sensitivity in response to methanol was 2326, 2857, and 833 (ppm/Hz) for PMMA, polystyrene, and P4VP channels, respectively. The sensitivity in response to toluene was 370, 357, and 370 (ppm/Hz) for PMMA, polystyrene and P4VP channels, respectively. It should be noted that the nature of this work was not to develop a more sensitive methanol or toluene sensor but was instead to analyze how predictive capabilities could improved with existing sensors. The key result of these sensitivities is the difference in magnitude between the responses to the analytes of interest. This difference is paramount when identifying candidate functional materials for multi-analyte, multi-channel sensing platforms. Initial ink screening should include identifying functional materials with different responses to the analytes of interest. This conclusion is directly applicable to sensing platforms beyond resonant mass sensors that use a change in an indicator value as a proxy for detection.

A key component in creating an effective sensor model lies in the training data and model terms chosen. Possible additional model terms such as higher-order or cross terms, as detailed in the results section, were included in the original versions of the regression model. However, when tested they were not significant ($\alpha$=0.01 ) predictors of frequency shift due to concentration changes. By choosing to include fewer terms in the model, the degrees of freedom increased. This allowed for more confidence in the detection claims.

The nature of this system of linear regression equations resulted in decisions regarding which equations should be included when performing the generalized inverse to determine the chamber concentration. It was found that to predict methanol concentrations, the data from channels functionalized with poly(4-vinylpyridine) was critical. If these channels were ignored the R2 for the methanol concentration did not exceed 0.44 in any other combination of model equations. If that data was used alone, the methanol concentration was predicted with an R2 of 0.30. However, if that data was used with any of the remaining channels' information, or pairs thereof, the R2 increased to 0.80–0.84 with the reference channel and poly(4-vinylpyridine) combination producing the highest R2 . This implies that the poly(4-vinylpyridine) was an effective predictor of methanol concentration but required an additional channel to assist in discerning the difference between toluene and methanol in

the chamber. This can be seen most clearly from the linear-regression coefficients in Table II. The methanol coefficient for the poly(4-vinylpyridine) equations is an order of magnitude higher than that for the other groupings. This distinction is a driving factor in the significant effect of these channels on predicting the methanol concentration accurately.

When considering the prediction of toluene, any channel type, or combination of channels, resulted in an R2 greater than or equal to 0.86 with the exception of a model including only polystyrene and polymethylmethacrylate, the two weakest predictors, which resulted in an R2 of 0.65. This indicates that the functional chemistries chosen were not selective to toluene and thus the response of a bare quartz crystal, the reference channel, was just as significant as the functional channels. This is demonstrated in Table II in which all of the toluene coefficients are of the same order of magnitude. This result informs the selection of functional chemistries. It is critical to implement functional materials that have significant responses to the analytes of interest and are distinct in their behavior to accurately predict the concentration of several analytes.

Figure 5 shows the oscillation frequency of 16 oscillators over time. Each subfigure represents a group of four oscillators with the same functional material. Ideally, these four channels would perform identically. However, it can be seen that the channels have similar qualitative trends but have significant quantitative spread in their data. This can be attributed, in part, to the error in droplet placement during functionalization. It was previously found that the devices used were most sensitive at their geometric center [22]. The location of the functional material was included in an iteration of the concentration/shift model; however, it did not prove to be a significant predictor. Namely, the material location is not the only element that this spread can be attributed to. It is hypothesized that there is a non-trivial effect of surface interactions with the various solvents used. As such, the same volume of deposited material may spread more or less depending on the surface/ink interactions. Additionally, this spread could result in non-uniform film thickness across devices. These added effects represent some of the device-to-device differences.

Due to the apparent spread in frequency shifts within an ink group, it is important to discern if the resonator has a random effect on the shift. To do so, the linear regression model with four ink groupings was expanded to 16 unique resonator equations. The least squares approach was then used to invert the equations and predict the methanol and toluene concentrations based on the same experimental data set. The result did not produce an improved concentration prediction. As such, it was concluded that the random resonator-based effects are not as significant as the ink effects. Moving forward, the ink-based groupings are sufficient to capture behavior with as few of the model equations as possible.

By implementing an array of oscillators functionalized with inkjet printing, a multi-channel sensing platform was created. The use of an FPGA-based frequency monitoring algorithm allowed for oscillation frequency data to be recorded every second and in parallel on all 16 channels. For practical field implementation, the FPGA approach can be miniaturized and integrated on chip for a fully deployable solution. The sensing platform and approach produced a low-cost, scalable sensing array for multiple analyte monitoring once per second. This allows the system to capture processes with non-trivial time scales. Furthermore, the redundant elements and multiple functional inks resulted in a linear regression model with high correlation coefficients, R2=0.81 and R2=0.99 for toluene and

methanol predictions, respectively. Through the use of least squares analysis, the model was able to be inverted and experimental shifts could be used to predict analyte concentrations. This step is meaningful because it brings the technology a step beyond claiming detection through demonstrated frequency shifts and towards building models to interpret the relationship between these shifts and possible analyte concentrations. Future sensor developments should keep practical sensing considerations in mind when developing platforms so the systems can be scalable and integrate with predictive methods for analyte concentrations.

## References


**1.**W. H. O. R. O. F. Europe, WHO Guidelines for Indoor Air Quality: Selected Pollutants, Geneva, Switzerland:World Health Organization. Regional Office for Europe, 2010.

**2.**L. Spinelle, M. Gerboles, G. Kok, S. Persijn and T. Sauerwald, "Review of portable and low-cost sensors for the ambient air monitoring of benzene and other volatile organic compounds", *Sensors*, vol. 17, no. 7, pp. 1520-1550, 2017.

**3.**S. De Vito, E. Massera, M. Piga, L. Martinotto and G. Di Francia, "On field calibration of an electronic nose for benzene estimation in an urban pollution monitoring scenario", *Sens. Actuators B Chem.*, vol. 129, no. 2, pp. 750-757, Feb. 2008.

**4.**M. Leidinger, T. Sauerwald, W. Reimringer, G. Ventura and A. Schütze, "Selective detection of hazardous VOCs for indoor air quality applications using a virtual gas sensor array", *J. Sensors Sensor Syst.*, vol. 3, no. 2, pp. 253-263, Oct. 2014.

**5.**A. Mirzaei, S. G. Leonardi and G. Neri, "Detection of hazardous volatile organic compounds (VOCs) by metal oxide nanostructures-based gas sensors: A review", *Ceram. Int.*, vol. 42, no. 14, pp. 15119-15141, Nov. 2016.

**6.**B. Szulczynski and J. Gebicki, "Currently commercially available chemical sensors employed for detection of volatile organic compounds in outdoor and indoor air", *Environments*, vol. 4, no. 1, pp. 21-36, 2017.

**7.**W. Miekisch, J. Herbig and J. K. Schubert, "Data interpretation in breath biomarker research: Pitfalls and directions", *J. Breath Res.*, vol. 6, no. 3, Sep. 2012.

**8.**N. Queralto, A. N. Berliner, B. Goldsmith, R. Martino, P. Rhodes and S. H. Lim, "Detecting cancer by breath volatile organic compound analysis: A review of array-based sensors", *J. Breath Res.*, vol. 8, no. 2, 2014.

**9.**M. Calleja, P. M. Kosaka, A. S. Paulo and J. Tamayo, "Challenges for nanomechanical sensors in biological detection", *Nanoscale*, vol. 4, no. 16, pp. 4925-4938, 2012.

**10.**A. D. Wilson, "Review of electronic-nose technologies and algorithms to detect hazardous chemicals in the environment", *Procedia Technol.*, vol. 1, pp. 453-463, Jan. 2012.

**11.**L. Spinelle, M. Gerboles, M. G. Villani, M. Aleixandre and F. Bonavitacola, "Field calibration of a cluster of low-cost available sensors for air quality monitoring—Part A: Ozone and nitrogen dioxide", *Sens. Actuators B Chem.*, vol. 215, pp. 249-257, Aug. 2015.

**12.**J. Toledo et al., "Out-of-plane piezoelectric microresonator and oscillator circuit for monitoring engine oil contamination with diesel", *Proc. SPIE*, vol. 9517, May 2015.

**13.**T. Manzaneque et al., "Piezoelectric MEMS resonator-based oscillator for density and viscosity sensing", *Sens. Actuators A Phys.*, vol. 220, pp. 305-315, Dec. 2014.

**14.**H. C. Hao et al., "Development of a portable electronic nose based on chemical surface acoustic wave array with multiplexed oscillator and readout electronics", *Sens. Actuators B Chem.*, vol. 146, no. 2, pp. 545-553, Apr. 2010.

**15.**F. Liu and M. Hossein-Zadeh, "Mass sensing with optomechanical oscillation", *IEEE Sensors J.*, vol. 13, no. 1, pp. 146-147, Jan. 2013.

**16.**K. Zeng, K. G. Ong, C. Mungle and C. A. Grimes, "Time domain characterization of oscillating sensors: Application of frequency counting to resonance frequency determination", *Rev. Sci. Instrum.*, vol. 73, no. 12, pp. 4375-4380, Dec. 2002.

**17.**J. Pettine, V. Petrescu, D. M. Karabacak, M. Vandecasteele, M. Crego-Calama and C. Van Hoof, "Power-efficient oscillator-based readout circuit for multichannel resonant volatile sensors", *IEEE Trans. Biomed. Circuits Syst.*, vol. 6, no. 6, pp. 542-551, Dec. 2012.

**18.**M. D. Valdes, I. Villares, J. Farina and M. J. Moure, "A FPGA-based frequency measurement system for high-accuracy QCM sensors", *Proc. 34th Annu. Conf. IEEE Ind. Electron.*, pp. 1707-1712, Nov. 2008.

**19.**A. Bietsch, J. Zhang, M. Hegner, H. P. Lang and C. Gerber, "Rapid functionalization of cantilever array sensors by inkjet printing", *Nanotechnology*, vol. 15, no. 8, pp. 873-880, Aug. 2004.

**20.**J. B. Chang et al., "Printable polythiophene gas sensor array for low-cost electronic noses", *J. Appl. Phys.*, vol. 100, no. 1, Jul. 2006.

**21.**V. Kumar et al., "Bifurcation-based mass sensing using piezoelectrically-actuated microcantilevers", *Appl. Phys. Lett.*, vol. 98, no. 15, Apr. 2011.

**22.**N. Bajaj, J. F. Rhoads and G. T.-C. Chiu, "Characterizing the spatially dependent sensitivity of resonant mass sensors using inkjet deposition", *J. Dyn. Syst. Meas. Control*, vol. 139, no. 11, Nov. 2017.

**23.**B. E. DeMartini, J. F. Rhoads, M. A. Zielke, K. G. Owen, S. W. Shaw and K. L. Turner, "A single input-single output coupled microresonator array for the detection and identification of multiple analytes", *Appl. Phys. Lett.*, vol. 93, no. 5, Aug. 2008.